Available online at www.sciencedirect.com
SCIENCE DIRECT
Journal of Molecular Catalysis A: Chemical 253 (2006) 112–118
JOURNAL OF MOLECULAR CATALYSIS A: CHEMICAL
www.elsevier.com/locate/molcata

Enhanced photocatalytic activity of TiO_2 powder (P25) by hydrothermal treatment

Jiaguo Yu *, Huogen Yu, Bei Cheng, Minghua Zhou, Xiujian Zhao

State Key Laboratory of Advanced Technology for Material Synthesis and Processing, Wuhan University of Technology, Luoshi Road 122#, Wuhan 430070, PR China

Received 10 February 2006; accepted 14 March 2006
Available online 18 April 2006

Abstract

TiO_2 powder (P25) was hydrothermally treated in pure water at 150 °C for different times. The P25 powders before and after hydrothermal treatment were characterized with XRD, TEM, UV–vis, XPS and nitrogen adsorption–desorption isotherms. The results showed that a small amount of anatase was transformed into rutile phase and more aggregates of the TiO_2 crystallites formed after hydrothermal treatment, resulting in the decrease of specific surface area of the TiO_2 powders. The photocatalytic activity of the hydrothermally treated P25 powders was obviously higher than that of the P25 powder. This can be attributed to the formation of more hydroxyl groups in the surface of TiO_2. The more hydroxyl groups would generate more hydroxyl radicals, enhance the adsorption of O_2 molecules and reduce recombination of the photogenerated electrons and holes. Moreover, more hydroxyl was also beneficial to the activation of the rutile phase, leading to an enhanced photocatalytic activity.

Keywords: Hydrothermal treatment; TiO_2 powders; P25; Photocatalytic activity; Enhancement

1. Introduction

Heterogeneous photocatalysis, a new water and air purification technique, has attracted great attention in the past decade [1–6]. The advantage of this technique over the traditional wastewater treatment (such as chlorination, ozonolysis) is that a broad variety of compounds, such as phenol, 4-chlorophenol, trichloroethylene and chlorobenzene in wastewater, can be mineralized completely [7–9]. Among various oxide semiconductors, titania is a very important photocatalyst owing to its strong oxidizing power, non-toxicity and long-term photostability. Despite its great potential, the fast recombination rate of photogenerated electron–hole pairs on the surface or in the lattice of TiO_2 hinders the commercialization of photocatalytic oxidation technology [10]. The further improvement of photoactivity of TiO_2 is one of the most important tasks for the technique applications of heterogeneous photocatalysis. In recently years, many methods have been applied to improve the photocatalytic activity of TiO_2, including the doping of transition mental or non-mental ions [11,12], the deposition of noble metals [13,14], the surface sensitization of dyes [15,16] and the preparation of composite semiconductors [17,18].

It is well known that the photocatalytic activity of TiO_2 strongly depends on the preparing methods and post-treatment conditions, since they have a decisive influence on the chemical and physical properties of TiO_2 [19]. To enhance photocatalytic activity, usually, two principle post-treatment methods have been used to control the physicochemical properties of the TiO_2. On one hand, heat treatment was a useful method for the enhancement of photoactivity of TiO_2. Yu et al. [10] demonstrated an obvious increase of photocatalytic activity after thermal treatment of TiO_2 (P25) in air, and thought that the increase in photoactivity can be attributed to a catalyst surface with more adsorbed oxygen. Sato et al. [20] suggested that the higher photocatalytic activity of TiO_2 obtained after calcination could be ascribed to the releasing of lattice oxygen from TiO_2. Recently, we also found that high temperature heat-treatment could obviously enhance the photocatalytic activity of the TiO_2 thin films [19]. On the other hand, hydrothermal treatment technique, a low temperature technology for materials synthesis, was widely applied to prepare various materials. By changing the hydrothermal reaction conditions, such as reac-

* Corresponding author.
E-mail address: jiaguoyu@yahoo.com (J. Yu).

1381-1169/$ – see front matter © 2006 Elsevier B.V. All rights reserved.
doi:10.1016/j.molcata.2006.03.021

tion temperatures, pH values, reactant concentrations and molar ratios, additives and so forth, crystalline products with different compositions, structures and morphologies have been obtained [21,22]. Wang and Ying [23] prepared nanocrystalline anatase and rutile TiO_2 by hydrothermal treatment of the sol–gel-derived hydrous oxides. Yin et al. [24] obtained nanocrystallites of anatase and rutile titania with narrow particle-size distributions by hydrothermal treatment using amorphous titania as the precursors. Kontos et al. [25] reported the enhanced photocatalytic activity of the TiO_2 thin films by hydrothermal modification of the P25 powder. They concluded that the hydrothermal treatment of the TiO_2 (P25) induced modification to the film roughness, surface area, agglomerated particle size and hydroxyl content of the photocatalysts, affecting the photocatalytic efficiency.

P25 powder, composing of anatase and rutile, is widely studied and well known to have good photocatalytic activity. In this study, it was found that the photocatalytic activity of TiO_2 (P25) increased significantly after hydrothermal treatment. The reasons for the enhanced photocatalytic activity of TiO_2 were not different from those reported by Kontos et al. [25] and Yu et al. [10]. The influence of hydrothermal treatment on the microstructures of TiO_2 powders was studied by using XRD, UV–vis, TEM, XPS and nitrogen adsorption–desorption isotherms. The photocatalytic activity of the TiO_2 samples before and after hydrothermal treatment was evaluated by the photocatalytic oxidation of acetone. The reasons for the enhanced photocatalytic activity of the hydrothermally treated TiO_2 samples were discussed.

2. Experimental

2.1. Hydrothermal treatment of TiO_2 (P25)

P25 powder was kindly provided by Degussa. In a typical hydrothermal treatment process, 0.5 g of P25 powder was mixed with 80 ml of distilled water, followed by hydrothermal treatment of the mixture at 150 °C in a 100 ml Teflon-lined stainless steel autoclave for 1–72 h. After the hydrothermal post-treatment, the obtained suspensions were transferred into dishes. The dishes containing catalysts were dried at 100 °C to evaporate water and then cooled to room temperature to obtain the hydrothermally treated TiO_2 powders.

2.2. Characterization

The X-ray diffraction (XRD) patterns were obtained on a X-ray diffractometer (type HZG41B-PC) using Cu Kα irradiation at a scan rate (2θ) of 0.05° s^{-1} and were used to determine the identity of any phase present and their crystallite size. The accelerating voltage and the applied current were 15 kV and 20 mA, respectively. Crystallite size and shapes were observed using a transmission electron microscopy (TEM) (JEOL 1200EX, Japan). X-ray photoelectron spectroscopy (XPS) measurements were performed on the ESCALAB-210 spectrometer (Thermo VG Scientific, UK) with Mg Kα source. All the binding energies were referenced to the C 1s peak at 285.0 eV of the surface adventitious carbon. The UV–vis spectra were obtained on an UV–visible spectrophotometer (UV-2550, SHIMADZU, Japan). $BaSO_4$ was used as a reflectance standard in the UV–vis diffuse reflectance experiment. Nitrogen adsorption–desorption isotherms were obtained on an ASAP 2020 (Micromeritics Instruments, USA) nitrogen adsorption apparatus. All the samples were degassed at 80 °C prior to BET measurements. The Brunauer–Emmett–Teller (BET) specific surface area (S_{BET}) was determined by a multipoint BET method using the adsorption data in the relative pressure (P/P_0) range of 0.05–0.3. Desorption isotherm was used to determine the pore size distribution using the Barret–Joyner–Halender (BJH) method [26]. The nitrogen adsorption volume at the relative pressure (P/P_0) of 0.970 was used to determine the pore volume and the average pore size.

2.3. Measurement of photocatalytic activity

Acetone (CH_3COCH_3) is a common chemical that is used extensively in the industrial and domestic fields. Therefore, we chose it as a model contaminate chemical. The photocatalytic oxidation of acetone is based on the following reaction [27–29]:

$$CH_3COCH_3 + 4O_2 \rightarrow 3CO_2 + 3H_2O \quad (1)$$

The photocatalytic activity measurement of the TiO_2 samples was performed in a 15 L reaction reactor using the photocatalytic degradation of acetone with an initial concentration of 350 ± 20 ppm. The detailed experimental process has been reported elsewhere [29]. The TiO_2 photocatalysts were prepared by coating an aqueous suspension of TiO_2 samples onto three dishes with a diameter of ca. 7.0 cm. The dishes containing catalysts were dried at 100 °C and then cooled to room temperature before being used. The weight of the TiO_2 catalysts used for each experiment was kept at ca. 0.5 g. After the catalysts were placed in the reactor, a small amount of acetone was injected with a microsyringe into the reactor. The reactor was connected to a $CaCl_2$-containing dryer used for controlling the initial humidity in the reactor. The acetone vapor was allowed to reach adsorption–desorption equilibrium with catalysts in the reactor prior to UV light irradiation. Integrated UV intensity in the range of 310–400 nm striking the coatings, measured with a UV radiometer (Model: UV-A, made in Photoelectric Instrument Factory of Beijing Normal University), was 2.5 mW/cm^2, while the peak wavelength of UV light was 365 nm. The concentration analysis of acetone, carbon dioxide and water vapor in the reactor was conducted on line with a Photoacoustic IR Multigas Monitor (INNOVA Air Tech Instruments Model 1312). The photocatalytic activity of the TiO_2 samples can be quantitatively evaluated by comparing the apparent reaction rate constants. The photocatalytic oxidation of acetone is a pseudo-first-order reaction and its kinetics may be expressed as follows: $\ln(C_0/C) = kt$ [28,29], where k is the apparent reaction rate constant, C_0 and C are the initial concentration and the reaction concentration of acetone, respectively.

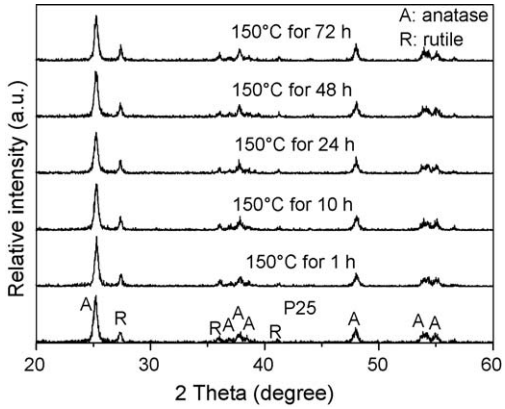

Fig. 1. XRD patterns of the TiO_2 powders hydrothermally treated at 150 °C for 1–72 h.

3. Results and discussion

3.1. Phase structures and crystallite sizes

The effect of hydrothermal treatment time on phase structures was studied using XRD. Fig. 1 shows the XRD patterns of TiO_2 powders before and after hydrothermal treatment for various times, indicating that all the samples were composed of both rutile and anatase phases. Further observation shows that the relative intensities of anatase and rutile diffraction peaks are different for the TiO_2 powders obtained at different hydrothermal treatment times. According to the following equation [21,30]:

$$f_r = \frac{1.26 I_r}{I_a + 1.26 I_r} \quad (2)$$

the mass fraction of rutile (f_r) in each sample can be calculated by measuring the intensities of the strongest (1 1 0) and (1 0 1) diffraction peaks of rutile (I_r) and anatase (I_a), respectively. The results are listed in Table 1. It can be seen that the mass fraction of rutile phase slightly increases with increasing hydrothermal treatment time. Prior to hydrothermal treatment, the mass fraction of rutile was ca. 22.4%. After hydrothermal treatment for 72 h, the content of rutile reached ca. 29.6%. Therefore, it is reasonable to suggest that a small amount of anatase phase was transformed into rutile TiO_2. Usually, the temperature of phase transformation from anatase to rutile depends on the particle size, morphologies of crystals and the addition of additives [31].

Table 1
Effects of hydrothermal treatment time on the phase structure, BET specific surface area (S_{BET}) and pore parameters of TiO_2 samples

Samples	W_R (%)	W_A (%)	E_g (eV)	S_{BET} (m^2/g)	Pore volume (cm^3/g)	Pore size (nm)
P25	22.4	77.6	3.35	49.3	0.09	8.3
1 h	24.0	76.0	3.30	47.5	0.20	17.1
10 h	28.0	72.0	3.25	46.3	0.23	18.4
24 h	28.6	71.4	3.21	45.0	0.23	18.8
48 h	29.5	70.5	3.17	43.6	0.24	20.3
72 h	29.6	70.4	3.16	43.2	0.26	23.4

As can be seen from the TEM image (Fig. 2a), the P25 powder shows a wide particle size distribution ranging from 10 to 60 nm. Moreover, some small particles with diameters of less than 10 nm were also observed. In this case, it seems that the crystallite size of the TiO_2 is the most important factor affecting the phase transformation. In the solution system, it has been reported that anatase has a critical size before its disappearance (complete phase transformation) [31]. Therefore, it is deduced that the increase of rutile might be attributed to the decrease of smaller anatase TiO_2 crystallites in the P25 powders. Also, smaller crystallites results in more defects in the crystal structure compared to the larger crystals [32]. This means that the number of potential crystallization nucleation sites for rutile was more in the samples with smaller crystallite size [32]. Furthermore, the phase transformation from anatase to rutile would be promoted by the presence of rutile phase [31]. Therefore, it is reasonable to conclude that the increasing rutile was formed via the consumption of anatase as a titania source. However, it should be noted that the increasing fraction of rutile would decrease with increasing hydrothermal treatment time. As shown in Table 1, the content of rutile has no obvious change when hydrothermal treatment time is larger than 48 h. This also indicates the existence of a critical crystallite size for the anatase to rutile phase transformation at a given temperature.

The TEM images of TiO_2 powders before and after hydrothermal treatment are shown in Fig. 2, indicating that the crystallite size has not an obvious change after hydrothermal treatment. However, more aggregates of TiO_2 crystallites were clearly observed after hydrothermal treatment for 10 h (Fig. 2b). The formation of more aggregates may be related to the change of surface properties of the TiO_2 crystallites (see below).

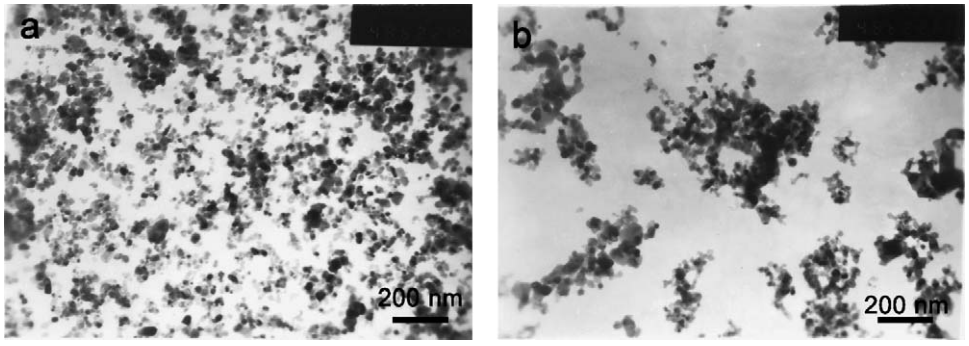

Fig. 2. TEM images of the TiO_2 powders (a) before and (b) after hydrothermal treatment at 150 °C for 10 h.

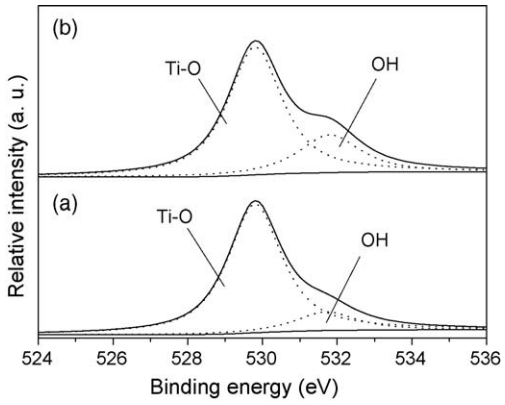

Fig. 3. High-resolution XPS spectra of O 1s region for the TiO_2 powders (a) before and (b) after hydrothermal treatment at 150 °C for 10 h.

3.2. Content of hydroxyl groups

IR spectroscopy is usually applied for monitoring the surface hydroxyl of various samples. However, it is difficult to distinguish the physically adsorbed water and the chemically adsorbed water (surface hydroxyl). It is well known that XPS is a surface probe detecting electrons that are generated from a depth of a few nm on the surface of sample. In this study, XPS analysis was used to study the identification of elements and their chemical state for the TiO_2 samples before and after hydrothermal treatment. The XPS survey spectra for the TiO_2 powders before and after hydrothermal treatment indicated that the powder was mainly composed of the Ti and O elements, and a small amount of C element was also observed, which was due to the adventitious hydrocarbon from the XPS instrument itself.

Fig. 3 shows the high-resolution XPS spectra of O 1s region for TiO_2 powders before and after hydrothermal treatment for 10 h. The O1s region is decomposed into two contributions. The main contribution is attributed to Ti–O in TiO_2, and the other minor peak can be ascribed to the OH on the surface of TiO_2 [19]. Although some H_2O is easily adsorbed on the surface of TiO_2 particles during the hydrothermal treatment and preparation of the TiO_2 samples, the physically absorbed H_2O on the TiO_2 is easily desorbed under the ultrahigh vacuum condition of the XPS system. Therefore, the hydroxyl on the surface can be attributed to the Ti–OH on the surface of TiO_2 samples. Table 2 lists the results of curve fitting of XPS spectra for the TiO_2 powders before and after hydrothermal treatment for 10 h. It can be seen from Table 2 that the content of hydroxyl groups on the surface of the TiO_2 powders has an obvious increase after hydrothermal treatment. Prior to hydrothermal treatment, the content of hydroxyl groups was ca. 10.8%. After hydrothermal treatment for 10 h, the mass fraction of hydroxyl groups reached ca. 24.9%. The obvious increase of hydroxyl groups may be related to the destruction of Ti–O–Ti and the formation of Ti–OH on the surface of TiO_2 crystallites under the hydrothermal conditions. The result was in good agreement with that reported by Kontos et al. [25]. On the other hand, the increase of hydroxyl group density would decrease the flow properties and the dispersion of particles [33], which led to an obvious aggregation of TiO_2 crystallites, as shown in Fig. 2b.

Table 2
Results of curve fitting of high-resolution XPS spectra for the O 1s region of TiO_2 samples before and after hydrothermal treatment

Samples	O 1s (Ti–O)	O 1s (OH)
P25		
E_b (eV)	529.9	531.8
fwhm	1.7	1.9
r_i (%)	89.2	10.8
10 h		
E_b (eV)	529.9	531.8
fwhm	1.7	1.9
r_i (%)	75.1	24.9

3.3. Light absorption characteristics

Hydrothermal treatment obviously affects the light absorption characteristics of the TiO_2, as shown in Fig. 4. A significant increase in the absorption at wavelengths less than 400 nm can be assigned to the intrinsic band gap absorption of TiO_2 [12,13]. Therefore, a slightly red shift indicated the decrease of band gap energies for the hydrothermally treated TiO_2 powders. The smaller band gap energy means a wider response range of the TiO_2 sample, and the sample can absorb more photons. This would contribute to an enhanced photocatalytic activity. To further explore the effect of hydrothermal treatment time on the absorption edge, the direct band gap energy can be estimated from a plot of $(h\nu\alpha)^2$ versus photo energy ($h\nu$). The relation between the absorption coefficient (α) and photon energy ($h\nu$) can be written as $\alpha = B_d(h\nu - E_g)^{1/2}/h\nu$, where B_d is absorption constants for direct transitions [34,35]. The plots of $(\alpha h\nu)^2$ versus $h\nu$ are presented in Fig. 5. The intercept of the tangent to the plot will give a good approximation of the direct band gap energies of the samples. The band gap energies of the TiO_2 powders before and after hydrothermal treatment were shown in Table 1. For all the TiO_2 powders, the direct band gap energies are between 3.16 and 3.35 eV, which is very close to 3.22 eV for the experimental nanopowders and the calculated value of 3.45 eV [35]. With increasing hydrothermal treatment time, the

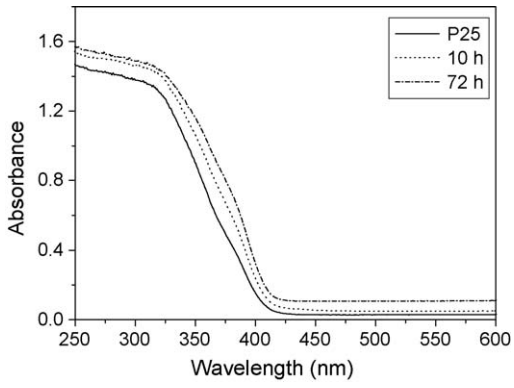

Fig. 4. UV–vis spectra of the TiO_2 powders (P25) before and after hydrothermal treatment at 150 °C for 10 and 72 h.

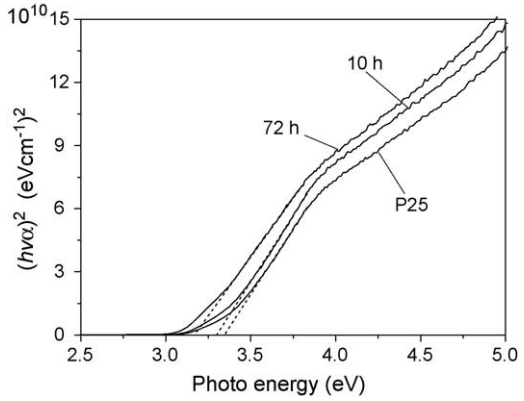

Fig. 5. Plots of $(h\nu\alpha)^2$ vs. photon energy for the TiO_2 powders (P25) before and after hydrothermal treatment at 150 °C for 10 and 72 h.

band gap energies of the TiO_2 samples decreased. The different band gap energies might be attributed to the difference in the surface microstructure, composition and phase structure in the TiO_2 powder [13].

3.4. S_{BET} and pore structures

Fig. 6 shows the nitrogen adsorption–desorption isotherms and their corresponding pore size distributions of TiO_2 powders before and after hydrothermal treatment for 10 h. It can be seen that all the samples show a type H3 hysteresis according to BDDT classification [26], indicating the presence of mesopores (2–50 nm). Moreover, the observed hysteresis approaches to $P/P_0 = 1$, suggesting the presence of large pores (>50 nm) [36]. The pore size distributions (inset) indicate a wide pore size distribution range from 2 to over 100 nm. In fact, P25 powder, produced through hydrolysis of $TiCl_4$ in a hydrogen flame [37], does not contain pores in each TiO_2 crystallites. Therefore, the formation of the pore structures in the samples could be attributed to the aggregations of TiO_2 crystallites. Also, it was reported that the average pore diameter coincides with the TiO_2 crystallite size and the average pore size increased with an increase in the crystallite size of titania powders [38]. Accordingly, the decrease of pore volume located at 2–10 nm for the

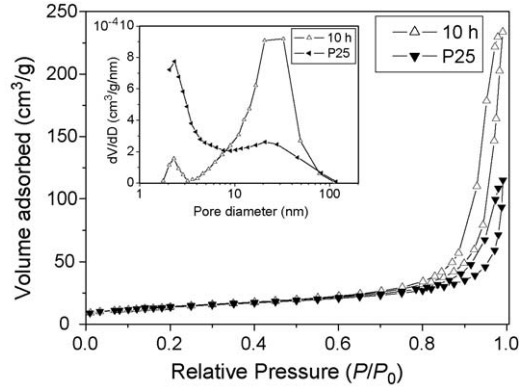

Fig. 6. The nitrogen adsorption–desorption isotherms and their corresponding pore size distributions (inset) of the TiO_2 powders (P25) before and after hydrothermal treatment at 150 °C for 10 h.

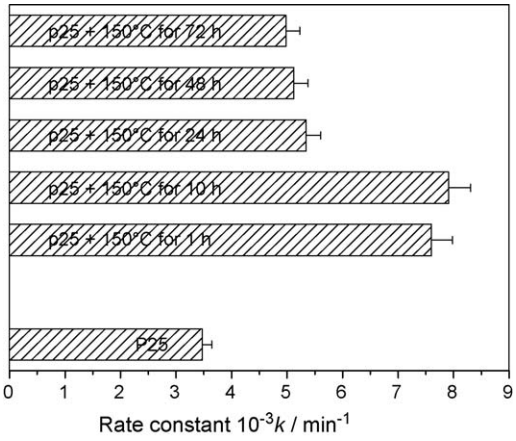

Fig. 7. The dependence of apparent rate constants of the TiO_2 powders on the hydrothermal treatment time.

hydrothermally treated TiO_2 samples indicated the decrease of smaller TiO_2 crystallites (<10 nm). This is in good agreement with the XRD analysis in which smaller anatase crystallites was transformed into rutile phase. Simultaneously, there was an obvious increase for the pore volume of larger pores (10–100 nm) after hydrothermal treatment, which can be ascribed to the formation of more aggregates of larger TiO_2 crystallites, as shown in TEM image (Fig. 2b). Textural parameters derived from the nitrogen adsorption–desorption isotherm data are summarized in Table 1. Compared with the P25 precursor, the S_{BET} of the hydrothermally treated TiO_2 samples slightly decreases, while the pore volume and the average pore size increase due to the formation of more aggregates of larger TiO_2 crystallites. In addition, the phase transformation of small anatase crystallites to rutile may also contribute to the decrease of S_{BET} and the increase of pore volume and average pore size.

3.5. Photocatalytic activity

Degussa P25 is a well-known and widely investigated photocatalyst due to its high activity for many kinds of photocatalytic reaction. It has been found that there is a positive interaction between anatase and rutile TiO_2 particles in Degussa P25 powders, which enhances the electron–hole separation and increases the total photocatalytic activity [39,40]. The mixing of an active oxidizing phase (anatase) with a comparatively inactive phase (rutile) could produce a kind of photocatalysts with unusually high activity [9,41]. The intimate contact between two phases might be sufficient to enhance the separation of photogenerated electrons and holes and result in the high photocatalytic activity of TiO_2 [37]. In this study, the P25 powders used were uniformly coated onto the surface of dishes, which would result in a good contact between anatase and rutile particles. Therefore, it was reasonable to conclude that a mixed effect between anatase and rutile would exist in our all the prepared samples for the photocatalytic reactions. However, it should be noted that there is an obvious enhancement in the photoactivity of the TiO_2 powders after hydrothermal treatment (Fig. 7). Especially, the apparent rate constant of the TiO_2 powders hydrothermally treated for

10 h is greater than that of P25 by more than two times. Therefore, it is suggested that in addition to the mixed effect of anatase and rutile phases, there must be some other factors enhancing the photocatalytic activity of the hydrothermally treated TiO_2 samples.

In the field of semiconductor photocatalysis, it is widely accepted that adsorbed molecular oxygen acts as a photogenerated electron acceptor, and the water or hydroxyl group reacts with the photogenerated hole to produce hydroxyl radical. The usually accepted mechanism of photocatalytic oxidation for TiO_2 is as follows [9,42].

$$TiO_2 + h\nu \rightarrow e^- + h^+ \quad (3)$$

$$e^- + h^+ \rightarrow \text{heat} \quad (4)$$

$$e^- + O_2 \rightarrow O_2^- \quad (5)$$

$$h^+ + OH \rightarrow {}^\bullet OH \quad (6)$$

The formation of O_2^- species has been monitored with chemiluminescence probing and the hydroxyl radical has also been detected by ESR spin trapping [42–45]. The O_2^- and $^\bullet OH$ can act as active species for the photodegradation of acetone. Therefore, the effective separation of electron–hole pairs, or the enhanced photodegradation of acetone can be promoted by the increase in the concentration of surface hydroxyl groups and adsorbed molecular oxygen. In this study, after hydrothermal treatment, there is not an obvious change of S_{BET}, pore volume, crystallization and crystallite size, while the content of hydroxyl groups increase significantly. Therefore, the enhanced photocatalytic activity may be related to the increasing number of hydroxyl groups on the surface of TiO_2.

It can be seen from the above results that the hydrothermal treatment led to a change in the surface physicochemical properties of the TiO_2 samples, which in turn affected the photocatalytic activity of the TiO_2 powders. It had been proved that the hydroxyl groups have a significant effect on the photocatalytic activity of the samples and the decrease of surface hydroxyl groups has a detrimental effect on the charge separation [46]. In photoelectrochemical cells, the surface hydroxyls could mediate electron transfer from the TiO_2 surface to electron acceptors [47]. Boonstra and Mutsaers [48] demonstrated a linear relation between the amount of adsorbed oxygen and the number of hydroxyl groups on the TiO_2 surface, and found that the amount of oxygen on the surface of TiO_2 decreased with decreasing amount of hydroxyls by calcination. Therefore, it is reasonable to conclude that the increase of amount of hydroxyl after hydrothermal treatment not only increase the trapping sites for photogenerated holes, but also can increase the trapping sites for photogenerated electrons by adsorbing more molecule oxygen. This results in more hydroxyl radicals to participate the photocatalytic reaction. Moreover, the increase of hydroxyl amount can enhance the transfer rate of photogenerated electron to O_2, leading to a decrease in the recombination rate of electron–hole pairs [47]. All these are beneficial to enhancing the photocatalytic activity of the TiO_2 samples. Ding et al. [7] also reported a similar result. In their study, the amount of the surface-adsorbed water and hydroxyl groups has an important effect on the photocatalytic activity of the samples with different anatse-to-rutile ratios, and the reduction of surface adsorbed water and hydroxyl groups resulted in the drop of phtocatalytic activity.

Another important fact for the enhanced photocatalytic activity may be the fact that the hydrothermal treatment could activate the rutile phase in the TiO_2 powder, which allows the rutile TiO_2 to participate the photocatalytic reaction. Owing to the higher activity of pure anatase compared to rutile, anatase is conventionally considered to be the active component in the mixed-phase catalysts, while rutile was regarded to serve passively as an electron sink [40]. However, it was reported that the lab-made rutile showed a good activity due to the existence of a large amount of hydroxyl groups [46]. On the contrary, the rutile obtained at a high temperature is inactive owing to a limited hydroxyl content. In fact, the P25 is produced through a high temperature hydrolysis of $TiCl_4$ in a hydrogen flame [37]. An irreversible dehydration would occur and the number of hydroxyl groups on the surface of rutile phase was scarce. Therefore, the contribution of rutile to the total photoactivity of the P25 will be very limited in addition to the mixed effect. Usually, The poor photocatalytic activity of rutile was proposed due to its higher electron–hole recombination rate, a smaller amount of reactants and hydroxyl adsorbed to its surface [8]. After hydrothermal treatment, there is an obvious increase in hydroxyl content on the surface of the samples (Fig. 4). It seems that hydrothermal treatment process activated the rutile TiO_2 by increasing the hydroxyl groups on the rutile TiO_2 surface. To further confirm the effect of hydrothermal treatment on the photoactivity of rutile phase, a set of contrast experiment was carried out. The as-prepared rutile (confirmed by XRD analysis) was hydrothermally treated at 150 °C for 10 h under the identical experimental conditions. The results indicated that the hydrothermally treated rutile showed a slightly higher photocataliytic activity than the as-prepared rutile TiO_2 precursor, thought the two kinds of rutile TiO_2 exhibited poor photoactivity. Tsai and Cheng [49] also demonstrated that the photocatalytic activity of the as-prepared rutile was ascribed to a large amount of hydroxyl groups present on the TiO_2 surface. Sclafani et al. [46] attributed the high activity of lab-made rutile to its large amount of hydroxyl groups on the surface, and proposed that they might trap the holes in the valence band and enhance the chemisorption of O_2 molecules in the conduction band. The hydroxyl groups on the surface of rutile promote the transfer of electron–hole pairs and reduce their combination rate. Moreover, the photocatalytic activity of pure rutile particles can be also enhanced due to the presence of a small amount of anatase phase remained in the TiO_2 powders [50].

With further increase in the hydrothermal treatment time from 10 to 72 h, the photocatalytic activity of the TiO_2 samples decreased. However, the apparent rate constants of all the hydrothermally treated TiO_2 powders were also higher that that of P25. This further confirmed that the hydroxyl groups play a critical role in the photocatalytic oxidation reaction of acetone despite the decrease of S_{BET} and the formation of more aggregates.

4. Conclusions

Hydrothermal treatment exhibits a marked influence on the microstructures and photocatalytic activity of the P25 (TiO_2) powders. After hydrothermal treatment, the BET specific surface areas of the P25 (TiO_2) powders decrease and rutile content increases. Meanwhile, the amount of hydroxyls on the surface of the TiO_2 powders obviously increased. The photocatalytic activity of the hydrothermally treated P25 powders was higher than that of the P25 powder by a factor of more than two times. This can be attributed to the formation of more hydroxyl groups on the surface of TiO_2.

Acknowledgements

This work was partially supported by the National Natural Science Foundation of China (50272049 and 20473059) and KPCME (106114). This work was also financially supported by the Excellent Young Teachers Program of MOE of China and Project-Sponsored by SRF for ROCS of SEM of China.

References

[1] M.R. Hoffmann, S.T. Martin, W. Choi, D.W. Bahnemann, Chem. Rev. 95 (1995) 69.
[2] M.A. Fox, M.T. Dulay, Chem. Rev. 93 (1993) 341.
[3] J. Zhao, T. Wu, K. Wu, K. Oikawa, H. Hidaka, N. Serpone, Environ. Sci. Technol. 32 (1998) 2394.
[4] F.B. Li, X.Z. Li, Appl. Catal. A 228 (2002) 15.
[5] J.G. Yu, X.J. Zhao, Q.N. Zhao, Thin Solid films 379 (2000) 7.
[6] H.G. Yu, S.C. Lee, C.H. Ao, J.G. Yu, J. Cryst. Growth 280 (2005) 612.
[7] Z. Ding, G.Q. Lu, P.F. Greenfield, J. Phys. Chem. B 104 (2000) 4815.
[8] S.J. Kim, H.G. Lee, S.J. Kim, J.K. Lee, E.G. Lee, Appl. Catal. A 242 (2003) 89.
[9] A.L. Linsebigler, G. Lu, J.T. Yates Jr., Chem. Rev. 95 (1995) 735.
[10] J.C. Yu, J. Lin, D. Lo, S.K. Lam, Langmuir 16 (2000) 7304.
[11] F.B. Li, X.Z. Li, C.H. Ao, S.C. Lee, M.F. Hou, Chemosphere 59 (2005) 787.
[12] J.C. Yu, J.G. Yu, W.K. Ho, Z.T. Jiang, L.Z. Zhang, Chem. Mater. 14 (2002) 3808.
[13] J.G. Yu, J.F. Xiong, B. Cheng, S.W. Liu, Appl. Catal. B 60 (2005) 211.
[14] I.M. Arabatzis, T. Stergiopoulos, M.C. Bernard, D. Labou, S.G. Neophytides, P. Falaras, Appl. Catal. B 42 (2003) 187.
[15] J. He, J. Zhao, T. Shen, H. Hidaka, N. Serpone, J. Phys. Chem. B 101 (1997) 9027.
[16] M. Stylidi, D.I. Kondarides, X.E. Verykios, Appl. Catal. B 40 (2003) 271.
[17] W.K. Ho, J.C. Yu, J. Lin, J.G. Yu, P.S. Li, Langmuir 20 (2004) 5865.
[18] I. Bedja, P.V. Kamat, J. Phys. Chem. 99 (1995) 9182.
[19] J.G. Yu, H.G. Yu, B. Cheng, X.J. Zhao, J.C. Yu, W.K. Ho, J. Phys. Chem. B 107 (2003) 13871.
[20] S. Sato, T. Kadowaki, K. Yamaguti, J. Phys. Chem. 88 (1984) 2930.
[21] M. Wu, J. Long, A. Huang, Y. Luo, Langmuir 15 (1999) 8822.
[22] H.M. Cheng, J.M. Ma, Z.G. Zhao, L.M. Qi, Chem. Mater. 7 (1995) 663.
[23] C.C. Wang, J.Y. Ying, Chem. Mater. 11 (1999) 3113.
[24] H. Yin, Y. Wada, T. Kitamura, S. Kambe, S. Murasawa, H. Mori, T. Sakata, S. Yanagida, J. Mater. Chem. 11 (2001) 1694.
[25] A.I. Kontos, I.M. Arabatzis, D.S. Tsoukleris, A.G. Kontos, M.C. Bernard, D.E. Petrakis, P. Falaras, Catal. Today 101 (2005) 275.
[26] K.S.W. Sing, D.H. Everett, R.A.W. Haul, L. Moscou, R.A. Pierotti, J. Rouquerol, T. Siemieniewska, Pure Appl. Chem. 57 (1985) 603.
[27] M.E. Zorn, D.T. Tompkins, W.A. Zeltner, M.A. Anderson, Appl. Catal. B 23 (1999) 1.
[28] J.G. Yu, J.C. Yu, M.K.P. Leung, W.K. Ho, B. Cheng, X.J. Zhao, J.C. Zhao, J. Catal. 217 (2003) 69.
[29] J.G. Yu, M.H. Zhou, B. Cheng, H.G. Yu, X.J. Zhao, J. Mol. Catal. A 227 (2005) 75.
[30] T.R.N. Kutty, R. Vivekanandan, P. Murugaraj, Mater. Chem. Phys. 19 (1988) 533.
[31] M. Wu, G. Lin, D. Chen, G. Wang, D. He, S. Feng, R. Xu, Chem. Mater. 14 (2002) 1974.
[32] J. Ovenstone, K. Yanagisawa, Chem. Mater. 11 (1999) 2770.
[33] R. Mueller, H.K. Kammler, K. Wegner, S.E. Pratsinis, Langmuir 19 (2003) 160.
[34] N. Serpone, D. Lawless, R. Khairutdinov, J. Phys. Chem. 99 (1995) 16646.
[35] X.H. Wang, J.G. Li, H. Kamiyama, M. Katada, N. Ohashi, Y. Moriyoshi, T. Ishigaki, J. Am. Chem. Soc. 127 (2005) 10982.
[36] C.C. Tsai, H. Teng, Chem. Mater. 16 (2004) 4352.
[37] A.K. Datye, G. Riegel, J.R. Bolton, M. Huang, M.R. Prairie, J. Solid State Chem. 115 (1995) 236.
[38] H. Hayashi, K. Torii, J. Mater. Chem. 12 (2002) 3671.
[39] R.I. Bickley, T. Gonzalez-Carreno, J.S. Lees, L. Palmisano, R.J.D. Tilley, J. Solid State Chem. 92 (1991) 178.
[40] D.C. Hurum, A.G. Agrios, K.A. Gray, T. Rajh, M.C. Thurnauer, J. Phys. Chem. B 107 (2003) 4545.
[41] D.C. Hurum, K.A. Gray, T. Rajh, M.C. Thurnauer, J. Phys. Chem. B 109 (2005) 977.
[42] T.A. Egerton, I.R. Tooley, J. Phys. Chem. 108 (2004) 5066.
[43] W.G. Wamer, J.J. Yin, R.R. Wie, Free Radical Biol. Med. 23 (1997) 851.
[44] T. Hirakawa, H. kominami, B. Ohtani, Y. Nosaka, J. Phys. Chem. B 105 (2001) 6993.
[45] T. Ohno, K. Sarukawa, K. Tokieda, M. Matsumura, J. Catal. 203 (2001) 82.
[46] A. Sclafani, L. Palmisano, M. Schiavello, J. Phys. Chem. 94 (1990) 829.
[47] P. Salvador, C. Gutierrez, Chem. Phys. Lett. 86 (1982) 131.
[48] A.H. Boonstra, C.A.H.A. Mutsaers, J. Phys. Chem. 79 (1975) 1694.
[49] S.J. Tsai, S. Cheng, Catal. Today 33 (1997) 227.
[50] T. Ohno, K. Tokieda, S. Higashida, M. Matsumura, Appl. Catal. A 244 (2003) 383.